Monte Carlo Studies of the Origins of the Compensation Effect in a Catalytic Reaction

Kristen A. Fichthorn

Department of Chemical Engineering, 164 Fenske Laboratory, The Pennsylvania State University, University Park, Pennsylvania 16802

W. Henry Weinberg*

Department of Chemical Engineering, University of California, Santa Barbara, California 93106

Received April 10, 1991. In Final Form: May 31, 1991

The compensation effect has been an engima to surface scientists since the beginning of the century. In this study, the origins of compensatory behavior in a model steady-state Langmuir–Hinshelwood reaction were clarified with Monte Carlo simulations. The compensation effect in this model system and analogous physical systems can be understood in terms of the temperature and coverage dependence of a distribution of activation energies for surface reaction (arising when adsorbate interactions are extant among reactants in the system) which must balance a narrow distribution of adsorption rates at steady state.

Introduction

In experimental determinations of rate coeficients of the Polanyi–Wigner form ($k = \nu_0 e^{-E/k_B T}$) for thermal desorption[1] and bimolecular reactions[1-3] of simple molecules on well-defined, single-crystalline transition-metal surfaces, it is often observed that the activation energy, E, and the preexponential factor, ν_0, vary markedly with the surface population (coverage) of adsorbed species. Changes in the activation energy with surface coverage are generally attributable to the existence of adsorbate–adsorbate interactions which alter the binding energy of both the adsorbed species and its transition state. The basis for the dependence of ν_0 on the surface coverage of the adsorbate has not been well-established, although, experimentally, this parameter has been observed to vary by up to 11 orders of magnitude with coverage.[4] From transition state theory, the general form of the preexponential factor is given by

$$\nu_0 = \frac{k_B T}{h} e^{\Delta S/k_B} \tag{1}$$

where ΔS is the change in entropy in going from the reactants to the transition state. The statistical mechanical entropy is defined by $\Delta S = k_B \ln(\Omega)$ where Ω is the ensemble partition function. Ω is generally comprised of vibrational terms plus a configurational term which is associated with the number of different ways to arrange an ensemble of adsorbates on a periodic single-crystalline surface of adsorption sites. Although considerable theoretical effort has been directed toward understanding possible coverage dependencies of ΔS, a recent survey[1] has indicated that current theoretical models which are based on this approach are incapable of reconciling the large variations in the preexponential factor that are observed experimentally. Moreover, these models have been unable to provide an explanation for the frequently observed *commensurable variation* of ν_0 and E with the adsorbate fractional surface coverage, a phenomenon known as the compensation effect.

If, in fact, the preexponential factor does not vary substantially with the fractional surface coverage of adsorbate, then it was conjectured[5] that perhaps analyses of these surface phenomena were not being conducted within the appropriate theoretical framework. Consider, for example, the rate expression typically assumed in the analysis of the kinetics of bimolecular Langmuir–Hinshelwood surface reactions, namely

$$r = k_r \theta_A \theta_B \tag{2}$$

where k_r has the Polanyi–Wigner form, and θ_i is the fractional surface coverage of reactant species i (i = A or B). Typically, the activation energy and preexponential factor are obtained from the slope and intercept, respectively, of an Arrhenius plot of $\ln(r/\theta_A\theta_B)$ vs $1/T$. Although the rate expression of eq 2 would be expected to be valid in the absence of lateral interactions among adsorbed surface reactants and in the event that sufficient "mixing" of surface species has occurred so that $r \propto \theta_A\theta_B$, it should be regarded as a limiting expression rather than a general form. Silverberg et al.[6,7] have observed that such a rate expression can be partitioned into two components: an "energetic" factor, which is comprised of the rate coefficient, and a "topological" factor, which reflects the spatial distribution of reactants on the catalytic surface. In the absence of adsorbate interactions, the rate coefficient is independent of the concentration and distribution of reactant coverage on the catalytic surface. However, with the presumption of adsorbate lateral interactions (a reasonable hypothesis, since evidence of adsorbate interactions can be observed experimentally in many systems), one may arrive at a rate expression of a different form than that of eq 2. Allowing the existence of adsorbate–adsorbate interactions, it is recognized that the rate coefficient is dependent on both the concentration and the spatial distribution of reactants on the catalytic surface. For example, with attractive nearest-neighbor interactions

(1) Seebauer, E. G.; Kong, A. C. F.; Schmidt, L. D. *Surf. Sci.* 1988, *193*, 417, and references therein.
(2) Engstrom, J. R.; Weinberg, W. H. *Surf. Sci.* 1988, *201*, 145.
(3) Madix, R. J. The Physics of Surfaces: Aspects of the Kinetics and Dynamics of Surface Reactions, Proceedings, A.I.P. Conference, La Jolla Institute, 1979.
(4) Taylor, J. L.; Ibbotson, D. E.; Weinberg, W. H. *J. Chem. Phys.* 1978, *69*, 4298.
(5) Kang, H. C.; Jachimowski, T. A.; Weinberg, W. H. *J. Chem. Phys.* 1990, *93*, 1418.
(6) Silverberg, M. H.; Ben-Shaul, A. *J. Chem. Phys.* 1985, *83*, 6501.
(7) Silverberg, M. H.; Ben-Shaul, A. *J. Chem. Phys.* 1987, *87*, 3178.

0743-7463/91/2407-2539$02.50/0

Table I. Parameters Characterizing Isolated Elementary Steps and Adsorbate Interactions of the Model System

elementary step	form of rate	parameters	adsorbate interactions
surface diffusion of A	eq 9	$\nu_{\parallel} = 1.8 \times 10^{12}\ s^{-1}$ $E_{B,0} = 17.0$ kcal/mol	$\epsilon_{AA} = 5.0$ kcal/mol $\epsilon_{AB} = 1.0$ kcal/mol
thermal desorption of B	eqs 5 and 6	$\nu_{0,d} = 10^{13}\ s^{-1}$ $E_{d,0} = 29.0$ kcal/mol	$\epsilon_{BB} = 2.0$ kcal/mol
surface reaction of an A–B pair	eq 11	$\nu_{0,r} = 10^{13}\ s^{-1}$ $E_{r,0} = 27.0$ kcal/mol	

among two reactant species, one would anticipate finding a greater number of nearest-neighbor reactant pairs than would arise in the absence of adsorbate interactions.[5] The increased propensity for reactant clustering with attractive adsorbate interactions would also increase the average activation energy for reaction in the ensemble because the activation barrier to reaction will be increased at particular locations at which reactants have clustered.[5] When adsorbate interactions occur, a more appropriate form of the bimolecular rate law has been proposed[5] and is given by

$$r = \nu\theta_{AB}\sum_i f_i e^{-E_i/k_BT} \tag{3}$$

In this expression, θ_{AB} is the total fractional surface coverage of reactant pairs and f_i is the fraction of reactant pairs whose local environment of adsorbed species dictates (through adsorbate lateral interactions) an activation energy for reaction, E_i. A rate expression of a similar form was put forth many years ago to account for compensatory behavior in terms of the intrinsic heterogeneity of a catalytic surface in the absence of adsorbate–absorbate interactions.[8]

It is obviously possible that the rate expression of eq 2 inadequately represents the more general form of eq 3 over wide ranges of temperature and fractional surface coverages of reactants. In general, thermodynamic and kinetic factors will cause changes in both the composition and the configuration of an overlayer of chemisorbed species when the temperature of the surface and the composition of the gas-phase species are varied. Among the thermodynamic influences is the tendency of a system to approach a minimum energy configuration (often through an ordering of adsorbed species) as the temperature of the surface is reduced. In fact, Johansson[9] and Zhdanov[10] have successfully modeled and interpreted the coverage dependence of the preexponential factor for the thermal desorption of CO from Ru(001) in terms of a dramatic reduction of the configurational entropy of the overlayer resulting from an order–disorder phase transition to the $(\sqrt{3}\times\sqrt{3})R30°$ configuration at a CO surface coverage of 1/3. Kinetic influences are those which prevent a system from attaining thermodynamic equilibrium at a certain temperature, pressure, and gas-phase composition. Considering, qualitatively, various thermodynamic and kinetic scenarios which could potentially exist during catalysis, it becomes patently obvious that the general validity of eq 2 is questionable.

In a series of Monte Carlo studies[11] conducted within the framework of the lattice-gas model, we have undertaken to assess the validity of bimolecular reaction rate expressions of the form eq 2 and to explore the ramifications of a distribution of rates given by eq 3 in systems having adsorbate–adsorbate interactions. The inherent advantage of a Monte Carlo approach lies in the fact that a distribution of the form of eq 3, as it is determined by a set of microscopic rate coefficients and adsorbate lateral interactions, can be obtained and measured precisely in numerical experiments. Our studies of the kinetics of a steady-state Langmuir–Hinshelwood reaction have shown that when the distribution of reactant pairs in eq 3 is temperature and coverage dependent and must balance a narrow distribution of adsorption rates, the parameters, ν_0 and E, obtained from Arrhenius plots do not, in general, reflect the microscopic surface averages. Furthermore, in accord with the earlier findings of Kang et al.,[5] we shall demonstrate that a sizable compensation effect can arise in apparent values of E and ν_0 obtained from Arrhenius plots as a consequence of these factors.

Model

The model catalytic reaction which we chose as the subject of our investigations is intended to convey general attributes of the CO oxidation reaction on a platinum single crystalline surface. The mechanism of this reaction is

$$\begin{aligned} A_{2,g} + 2S &\rightarrow 2A\text{–}S \\ B_g + S &\rightleftarrows B\text{–}S \\ A\text{–}S + B\text{–}S &\rightarrow AB_g + 2S \end{aligned} \tag{4}$$

Here, A represents oxygen, B represents CO, and S, a vacant site on the catalytic surface. A qualitative description of the CO oxidation reaction over platinum has risen from numerous studies of this perennial system.[12] Carbon monoxide is generally regarded as being quite mobile and maintaining an equilibrium with the gas phase. Oxygen, on the other hand, is relatively immobile, and its adsorption is essentially irreverisble at moderate surface temperatures. The surface reaction of chemisorbed CO and oxygen is also an essentially irreversible step, reflecting the relatively low binding energy of CO_2 to platinum substrates. Experimental studies of both CO[13–15] and O_2[16,17] adsorption on various platinum surfaces have revealed decreases in the heats of adsorption of these species with increasing coverage which are indicative of *repulsive* CO–CO and O–O interactions.

The integration of this general scenario into a Monte Carlo model first requires a definition of the rates of the various surface processes and an interpretation of the influence of adsorbate interactions on these rates. A set of parameters consistent with the qualitative description of the preceding section is summarized in Table I. A simplifying feature in the model is that B, because of its presumed rapid mobility and moderate heat of adsorption, should establish a minimum energy configuration on the

(8) Constable, F. H. *Proc. R. Soc. London, Ser. A* **1925**, *108*, 355.
(9) Johansson, P. K. *Chem. Phys. Lett.* **1979**, *65*, 366.
(10) Zhdanov, V. P. *Surf. Sci.* **1981**, *111*, L662.
(11) Fichthorn, K. A.; Weinberg, W. H. To be published.
(12) Engel, T.; Ertl, G. *Adv. Catal.* **1979**, *28*, 1.
(13) Ertl, G.; Neumann, M.; Streit, K. M. *Surf. Sci.* **1977**, *64*, 393.
(14) Seebauer, E. G.; Kong, A. C. F.; Schmidt, L. D. *Surf. Sci.* **1986**, *176*, 134.
(15) Norton, P. R.; Goodale, J. W.; Selkirk, E. B. *Surf. Sci.* **1979**, *83*, 189.
(16) Steininger, H.; Lehwald, S.; Ibach, H. *Surf. Sci.* **1982**, *123*, 1.
(17) Campbell, C. T.; Ertl, G.; Kuipers, H.; Segner, J. *J. Chem. Phys.* **1980**, *73*, 5862.

surface with respect to the A adatoms on the time scale of surface reaction and maintain equilibrium with gas-phase B. Hence, we determined the surface distribution of B by equating the gas phase and surface chemical potentials of B. For an unoccupied surface site having j nearest neighbor A's, the probability of finding a B was calculated via

$$P_{B,j} = \frac{1}{1 + \alpha e^{-E_{d,j}/k_B T}} \tag{5}$$

where

$$\alpha = \frac{\nu_{0,d}\,(2\pi m_B k_B T)^{1/2}}{p_{B,g} C} \tag{6}$$

and

$$E_{d,j} = E_{d,0} - j\epsilon_{AB} - (4 - j)P_{B,0}\epsilon_{BB} \tag{7}$$

In these expressionsm, $p_{B,g}$ is the partial pressure of B in the gas phase and C is a conversion factor of 10^{-15} cm^2/site. With B accounted for in this fashion, the task of the Monte Carlo algorithm was to model the dissociative adsorption, surface diffusion, and reaction of A.

The rate of direct dissociative adsorption of A_2 on a pair of surface sites (i,j) unoccupied by A was calculated via

$$r_{A_2,ads}(i,j) = \frac{p_{A_2} C}{(2\pi m_{A_2} k_B T)^{1/2}}(1 - P_{B,i})(1 - P_{B,j}) \tag{8}$$

where p_{A_2} is the partial pressure of gas-phase A_2 and $P_{B,i}$ and $P_{B,j}$ are given by eq 5–7. The rate of adatom hopping of an A chemisorbed on a site, i, to a nearest-neighbor site unoccupied by A, j, was calculated via

$$r_{A,diff}(i,j) = \nu_{\parallel} e^{-E_B(i,j)/k_B T}(1 - P_{B,j}) \tag{9}$$

Here, $\nu_{\parallel}$ is the frustrated translational frequency of an A adatom parallel to the surface, and $E_B(i,j)$ is the energy barrier to thermally activated diffusion. The energy barrier to surface diffusion was taken as the intersection of two harmonic potential energy curves characterizing the chemisorption of A in an initial (i) and final (j) state, i.e.

$$E_i = \tfrac{1}{2}k\xi^2 + (n_{AA}\epsilon_{AA} + n_{BA}\epsilon_{AB})_i$$

$$E_j = \tfrac{1}{2}k(\xi - \lambda)^2 + (n_{AA}\epsilon_{AA} + n_{BA}\epsilon_{AB})_j \tag{10}$$

Here, ξ is the one-dimensional coordinate for adatom hopping, and the force constant, k, is based on the bonding of an oxygen adatom to a platinum atom which leads to the value of $\nu_{\parallel}$ given in Table I. The lattice constant, λ, was taken as 2.7 Å—approximately the diameter of a platinum atom. Solution of these equations for diffusion of an isolated A atom leads to the zero-coverage barrier given in Table I. In eq 10, nearest-neighbor adsorbed species modify the zero-point energy levels of both the chemisorbed species and the transition state. The quantity n_{AA} is the number of nearest-neighbor A's to an A, and n_{BA} is the number of nearest-neighbor B's to an A. The latter quantity was calculated by generating a uniform random number, $r_n \in (0...1)$, for each unoccupied nearest-neighbor site to the initial and final state and comparing these to the probabilities of B chemisorption on these sites. If r_n was less than or equal to this probability for a particular site, then a B molecule was assigned to the site for the purpose of calculating the barrier.

The rate of surface reaction of an A on site i with a B on a nearest-neighbor site j was of the form

$$r_r(i,j) = 2\nu_{o,r} e^{-E_r(i,j)/k_B T} P_{B,j} \tag{11}$$

The activation energy for reaction $E_r(i,j)$ was calculated via

$$E_r = E_{r,0} - n_{AA}\epsilon_{AA} - n_{BB}\epsilon_{BB} - (n_{AB}\epsilon_{AB} + n_{BA}\epsilon_{BA}) \tag{12}$$

Here, n_{BB} is the number of nearest-neighbor B's and n_{AB} is the number of nearest-neighbor A's to the B molecule in the reaching pair. The quantities n_{BB} and n_{BA} were calculated with a procedure analogous to that for adatom hopping. Although the preexponential factor for reaction could vary with the local configuration of reactant pairs, we have chosen to assign a *constant value* (cf. Table I) to this parameter in our calculations so that any apparent variations of this parameter could be easily discerned.

Monte Carlo simulations of the model reaction were conducted on 32 × 32 and 64 × 64 square lattices with periodic boundary conditions. Since each of the elementary steps of dissociative adsorption, surface diffusion, and bimolecular surface reaction involved a nearest-neighbor pair of surface sites, the Monte Carlo algorithm was formulated as follows:

1. The total transition rate was calculated for each unique pair of nearest-neighbor sites. Possible transition rates for a pair of sites (i,j) (S is a surface site containing B with some probability, and A is a site occupied by an A) were the following: SS, adsorption (via eq 8); AS, SA, surface diffusion or reaction (the sum of eqs 9 and 11); AA, no transition possible (rate is zero).

2. The pair having the maximum transition rate, r_{max}, was identified and updated throughout the course of the simulation.

3. A pair of index k was chosen at random and its transition probability, p_k $(=r_k/r_{max})$ was compared to a uniform random number $r_n \in (0...1)$.

4. If r_n was less than or equal to p_k, then the transition was executed, the status of all pairs affected by the transition was updated, and time was incremented.

5. Steps 3 and 4 were repeated, ad infinitum, and various properties of the system were monitored over time.

The Monte Carlo sampling procedure that was utilized effectively simulated the model system as a Poisson process.[18] Consistent with the theory of Poisson processes was the time increment, τ_T, upon each successful trial, T

$$\tau_T = \frac{1}{\sum_{k=1}^{2N} r_{k,T}} \tag{13}$$

Here, $r_{k,T}$ is the total transition rate of pair k at trial T, and the summation runs over all the $2N$ unique nearest neighbor pairs of sites for a square lattice of N sites. Our sampling algorithm and methodology for incrementing time assured that the passage of *real time* was correctly maintained.[18]

Simulations were run for A_2 partial pressures ranging from 10^{-3} to 10^{-6} Torr and a B partial pressure of 10^{-6} Torr. Simulation temperatures ranged from 325 to 500 K. Since the steady-state rate of reaction was of interest in this study, it was necessary for us to ascertain that steady state had been achieved. Simulations were run, beginning with an empty lattice, until the fractional surface coverage of A, θ_A, established and maintained an apparently constant value. This steady-state value was confirmed with simulations beginning with a fractional surface

(18) Fichthorn, K. A.; Weinberg, W. H. *J. Chem. Phys.* **1991**, *95*, 1090.

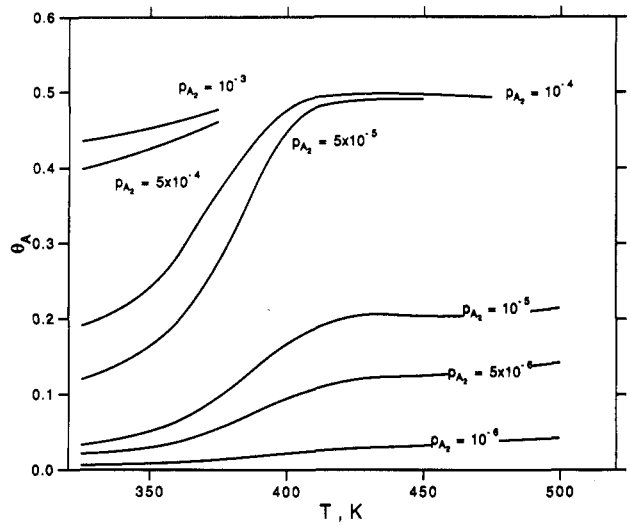

Figure 1. Isobars of reactant A_2 obtained at various temperatures and steady-state fractional surface coverages of A probed in our study. The pressures are in Torr.

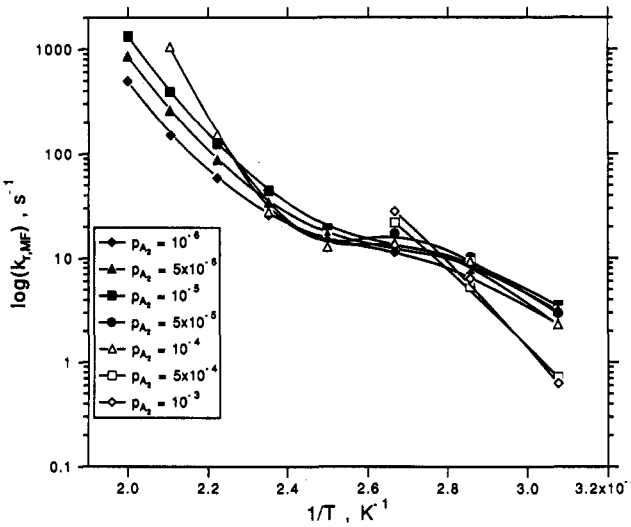

Figure 2. Arrhenius plots, parametric in the partial pressure of A_2, of the "mean-field" rate coefficient, $k_{r,MF}$, given by eq 15. The pressures are in Torr.

coverage of $\theta_A = 0.6$ (all steady-state coverages were substantially lower than this value) in which the coverage decreased to and maintained the same value. When the steady state had been determined, a long run comprising 20000–50000 reactions (simulated real times ranging from a few minutes to nearly an hour) was conducted and various statistics were measured. In addition, four shorter runs utilizing different random number sequences were conducted at the steady-state coverage to provide further confirmation of the results. Figure 1 depicts isobars of A_2 generated by the simulation at all temperatures and pressures probed in this investigation. Of central interest in this study was the simulated rate of reaction at various temperatures and partial pressures of A_2. We measured the rate in the simulations as the number of reactions, n_r, per pair occurring over a simulated time interval, Δt, i.e.

$$r_{rxn} = \frac{n_r}{2N\Delta t} \tag{14}$$

The rate of reaction was measured over the variable time interval, Δt, required for 20 reactions, and many such intervals were averaged at steady state. "Mean-field" rate coefficients, $k_{r,MF}$, were obtained from the average rate of

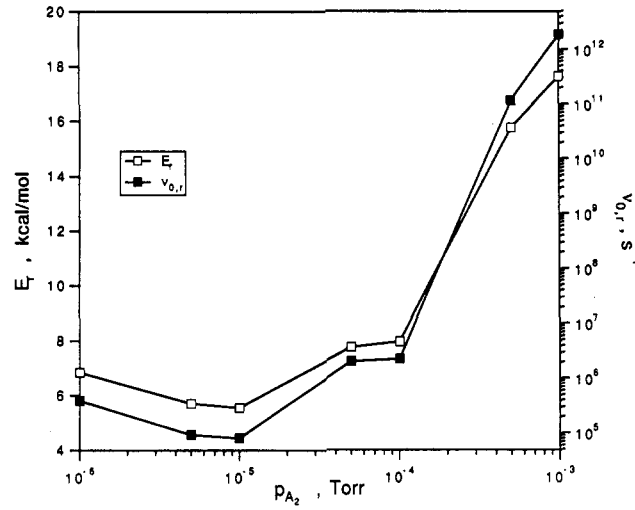

Figure 3. Activation energies and preexponential factors obtained from the slopes and intercepts of the Arrhenius plots of Figure 2 in the low temperature regime (T = 325–375 K).

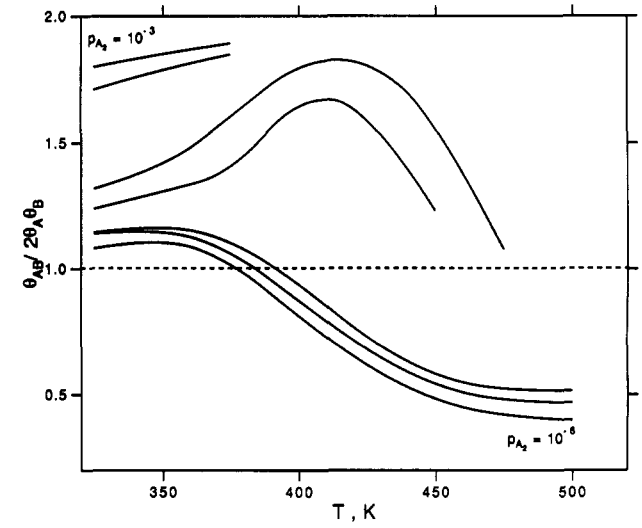

Figure 4. An assessment of the validity of the mean-field approximation for the model system. The quantities $\langle\theta_A\rangle$ and $\langle\theta_B\rangle$ were measured as time averages, and $\langle\theta_{AB}\rangle$ was calculated from eqs 16 and 17. The curves are parametric in the partial pressure of A_2 and follow an arithmetic order of the pressures probed in this study; cf. Figure 1. The pressures are in Torr.

reaction at a particular set of conditions through the relation

$$k_{r,MF} = \frac{\langle r_{rxn}\rangle}{2\langle\theta_A\rangle\langle\theta_B\rangle} \tag{15}$$

To ascertain the validity of the mean-field approximation, we measured the average fractional surface coverage of A–B pairs as

$$\langle\theta_{AB}\rangle = \frac{1}{4N}\sum_{(i,j)}\sigma_i p_{B,j} \tag{16}$$

where

$$\sigma_i = \begin{cases} 1, \text{ if site } i \text{ contains an A} \\ 0, \text{ otherwise} \end{cases} \tag{17}$$

The sum of eq 16 runs over all nearest-neighbor pairs (i,j) and introduces an extra factor of two in the denominator because of implicit double counting. Also of interest was the actual distribution of activation energies for pairs undergoing surface reaction. We recorded the activation

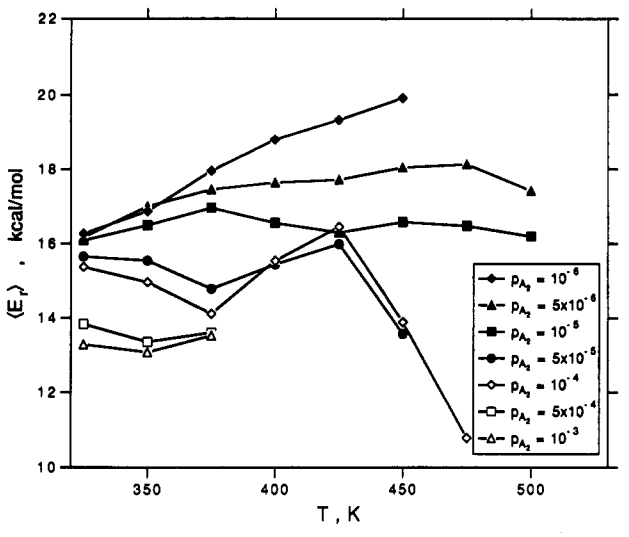

Figure 5. Activation energies measured as a frequency-weighted average over many surface reactions at all temperatures and pressures of this study. The pressures are in Torr.

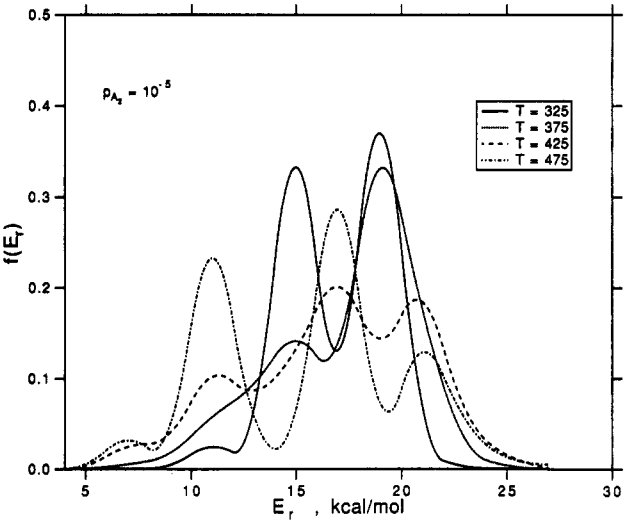

Figure 6. Frequency-weighted distribution of activation energies for reaction, as given by eq 18, at $p_{A_2} = 10^{-5}$ Torr for temperatures of 325, 375, 425, and 475 K. Although the distributions are, in actuality, discrete, they were represented as continuous distributions to facilitate their visual discernment.

energy upon each reaction of the model system and stored this frequency-weighted distribution and its mean for a given set of conditions. Figure 2 shows a series of Arrhenius plots of ln ($k_{r,MF}$) vs $1/T$ which are parametric in the partial pressure of A_2. These plots exhibit two apparent kinetic regimes, each with a compensatory trend. Figure 3 depicts the activation energies and preexponential factors obtained from the slopes and intercepts of the Arrhenius plots of Figure 2 in the low-temperature regime (T = 325–375 K) as a function of the partial pressure of A_2. Note that, although $\nu_{0,r}$ was a constant in the simulations (10^{13} s^{-1}), values of the preexponential factors obtained from the Arrhenius plots ranged over 7 orders of magnitude and in all cases were lower than 10^{13} s^{-1}. Figure 4 depicts the ratio of the actual fraction of A–B reactant pairs to the mean-field approximation of this quantity. It can be seen in this figure that the mean-field approximation is reasonable for the model system of this study. Clearly, the use of this approximation did not elicit the compensatory behavior shown in Figure 3.

Figure 5 depicts the frequency-weighted mean of the activation energy measured as an average over all pairs undergoing surface reaction at a particular set of conditions. A comparison of Figures 3 and 5 reveals that while the apparent activation energies determined from the Arrhenius plots increase with increasing partial pressure of A_2, the actual mean activation energies decrease with increasing A_2 pressure. The temperature dependence of the activation energies shown in Figure 5 provides an indication that the slopes of Arrhenius plots should be viewed with suspicion. Even at $p_{A_2} = 10^{-5}$ Torr, where the mean activation energy changes very little with temperature (cf. Figure 5), the actual and apparent activation energies are highly disparate (cf. Figures 3 and 5).

That the Arrhenius plots cannot, with any reasonable accuracy, recount activation energies such as those measured at $p_{A_2} = 10^{-5}$ Torr can be understood when the rate is viewed in terms of the parametrization of eq 3 which must balance a narrow distribution of direct, dissociative rates of A_2 adsorption at steady state.[11] Figure 6 shows the frequency-weighted distribution of activation energies for reaction obtained at $p_{A_2} = 10^{-5}$ Torr for four different temperatures. The relation of this distribution to the distribution of eq 3 is given by

$$f(E_r) = \frac{f_i e^{-E_{r,i}/k_B T}}{\sum_j f_j e^{-E_{r,j}/k_B T}} \qquad (18)$$

Although these distributions are, in acutality, discrete, they were approximated with continuous curves to facilitate their visual discernment. The energy distributions of Figure 6 are quite complex and, consistent with thermodynamic considerations, they tend to broaden and shift to lower activation energies (reflecting higher configurational energies of the ensemble at higher reactant coverages) as the temperature of the system is increased. Understanding the thermodynamic and kinetic factors contributing to the rtemperature and coverage dependence of distributions such as these is a central focus of our ongoing research.[11]

Conclusions

The issue of primary concern in this study was to demonstrate that there is a potentially significant error associated with approximating a rate comprised of a distribution of activation energies with an expression containing a single activation energy. As evidenced by our study, complex energy distributions of reactant pairs can arise when adsorbate–adsorbate interactions are extant. The temperature and coverage dependence of these distributions in balance with the rate of adsorption can render the Arrhenius construction completely meaningless and can furnish compensatory variation of the preexponential factor in substantial excess of the nominal variation prescribed by most theories. Experimentally reported preexponential factors which are either unusually large (e.g. $\geq 10^{16}$ s^{-1}) or unusually small (e.g. $\leq 10^{10}$ s^{-1}), and the activation energies associated therewith, should be viewed henceforth with appropriate caution.

Acknowledgment. This research was supported by the Department of Energy under Grant No. DE-FG03-89ER14048. K.A.F. thanks IBM for a postdoctoral research fellowship.